CHARACTERIZING CHANGES IN THE NOISE STATISTICS OF GNSS SPACE CLOCKS WITH THE DYNAMIC ALLAN VARIANCE

Lorenzo Galleani

Politecnico di Torino, Corso Duca degli Abruzzi 24, 10129 Torino, Italy

ABSTRACT

The dynamic Allan variance (DAVAR) is a tool for the characterization of precise clocks. Monitoring anomalies of precise clocks is essential, especially when they are employed onboard the satellites of a global navigation satellite system (GNSS). When an anomaly occurs, the DAVAR changes with time, its shape depending on the type of anomaly occurred. We obtain the analytic DAVAR for a change of variance in the clock noise, an anomaly with critical effects on the clock performances. This result is helpful when the clock health is monitored by observing the DAVAR.

Index Terms— Dynamic Allan variance, GNSS clocks, clock noise, clock anomaly, change of variance

1. INTRODUCTION

Precise clocks are the core of global navigation satellite systems (GNSSs). The user position is in fact estimated from the time of flight of the signals traveling from the satellites to the receiver. Therefore, an error in time implies an error in position, and precise clocks are used onboard satellites to reduce the positioning error. Common space clocks are cesium, rubidium, and hydrogen maser clocks. Atomic clocks are also used in ground stations to generate the system time, to which all space clocks are periodically synchronized.

Space clocks can experience anomalies due to several factors, such as radiations, temperature, aging, and sudden breakdowns. Understanding atomic clock anomalies is essential because of their negative effect on the positioning error, and for this reason they have attracted several investigators in the recent years. In [1], phase jumps, frequency jumps and shot-noise-type anomalies are detected and removed; in [2] clock frequency jumps are detected by using an approach based on energy; in [3]- [5] the Kalman filter is used to detect clock anomalies; in [6] the performances and anomalies of the clocks on-board the experimental Galileo satellites GIOVE-A and GIOVE-B are discussed; in [7] onboard measurements to detect and mitigate clock anomalies are studied.

We instead focus on variations in the statistics of the clock noise. Specifically, we consider changes of variance in the clock noise. Although this anomaly has received little attention, it is interesting for two main reasons. First, it can make the clock violate the specifications, which bound the maximum clock noise variance, with a negative effect on the clock predictability and, consequently, on the positioning error. Second, it might have a correlation with major clock failures. In Fig. 1 we show the behavior of a clock onboard the GPS satellite SVN30 for a few months of 2011. We see that the clock noise variance increases suddenly at approximately $t = 120$ days. Then, the clock is turned off, and after a block of missing data it is replaced by a new one, as confirmed by the corresponding GPS notice advisory to Navstar users.

We characterize how a change of variance in the clock noise impacts the clock stability, the fundamental quantity characterizing the performances of a precise clock. The IEEE [8] and ITU [9] standard definition of clock stability is the Allan variance [10], [11]. The Allan variance is a function of the interval τ on which the clock is observed. The smaller the Allan variance, the higher the clock stability and its performances in terms of predictability and, ultimately, of user positioning error.

Unfortunately, as our calculations show, the Allan variance averages out changes of variance in the clock noise, and therefore it cannot be used to characterize this type of anomaly. This goal can be achieved with the dynamic Allan variance (DAVAR) [12], [13], an extension of the Allan variance for the characterization of clocks affected by anomalies. The DAVAR is a surface function of time and the observation interval τ. When the clock behaves according to the specifications, the DAVAR is stationary with time. When an anomaly occurs, the shape of the DAVAR changes depending on the type of anomaly.

We obtain the analytic DAVAR for a sudden change in the clock noise variance. The result shows that the DAVAR clearly tracks the change of variance. In addition to characterizing how clock stability is affected by a change of variance, knowing the DAVAR for this type of anomaly is interesting for two reasons. First, it clarifies the shape of the DAVAR for a change of variance without the fluctuations naturally arising in the estimate obtained from measured data. This knowledge helps the operators which monitor the quality of space clocks in detecting and identifying clock anomalies. Second, it is useful for the design of anomaly detectors based on variations of the shape of the DAVAR surface [14]. We point out that the characterization of the change of variance presented

in this article is completely analytic, whereas in our previous works we have carried out numerical studies only. We also note that the presented result is part of a research line on the characterization of precise clock anomalies in the DAVAR domain. In [15], [16] we investigate in fact a series of common anomalies occuring in precise clocks, such as deterministic oscillations, phase jumps, and frequency jumps.

The article is organized as follows. In Sect. 2 we obtain the Allan variance and the DAVAR for a clock first with constant variance and then with a change of variance. In Sect. 3 we analyze the obtained DAVAR for the case of a change of variance.

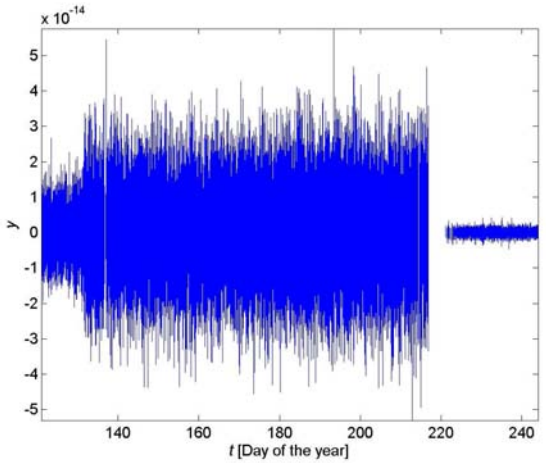

Fig. 1. A few months of data from the clock onboard GPS satellite SVN30. After an increase in variance approximately at $t = 120$ days, the clock is turned off and replaced by a new one.

2. THE DYNAMIC ALLAN VARIANCE OF A CHANGE OF VARIANCE

We define the time deviation $x(t)$ as the deviation of the clock reading $h(t)$ from a time reference $h_0(t)$,

$$x(t) = h(t) - h_0(t). \tag{1}$$

The corresponding (normalized) frequency deviation is

$$y(t) = \frac{dx(t)}{dt}. \tag{2}$$

The time and frequency deviations are fundamental quantities for the description of precise clocks [17]. Since they have the structure of noise, they are referred to as clock noise. We now consider two cases. First, the stationary case of a white frequency noise. Second, the nonstationary case of a white frequency noise whose variance increases suddenly at $t = 0$.

2.1. Constant variance

The noise components in the clock noise change depending on the clock type. A simple and effective model of the clock noise is a white frequency noise on the frequency deviation, defined as

$$y(t) = \xi(t), \tag{3}$$

where $\xi(t)$ is a white Gaussian noise with zero mean and autocorrelation function

$$R_\xi(t_1, t_2) = \delta(t_1 - t_2). \tag{4}$$

Typically, the available measurements are the sampled values $x[n] = x(nT_s)$ of the time deviation, where T_s is the sampling time. The corresponding discrete-time frequency deviation $y[n]$ is obtained as

$$y[n] = \frac{x[n] - x[n-1]}{T_s}. \tag{5}$$

By inverting (2), we can rewrite $y[n]$ as

$$y[n] = \frac{1}{T_s} \int_{(n-1)T_s}^{nT_s} y(t')dt'. \tag{6}$$

This result shows that the discrete-time frequency deviation $y[n]$ is obtained by averaging the corresponding continuous-time version $y(t)$.

The standard quantity for the characterization of clock noise is the Allan variance [8]-[11],

$$\sigma_y^2(\tau) = \frac{1}{2} \left\langle \Delta^2(t, \tau) \right\rangle, \tag{7}$$

where

$$\Delta(t, \tau) = \bar{y}(t + \tau) - \bar{y}(t), \tag{8}$$

the average frequency deviation on an observation interval τ is

$$\bar{y}(t) = \frac{1}{\tau} \int_{t-\tau}^{t} y(t')dt', \tag{9}$$

and $\langle\rangle$ is the averaging operator defined as

$$\sigma_y^2(\tau) = \frac{1}{2} \lim_{T' \to \infty} \frac{1}{T'} \int_{-T'/2}^{T'/2} \Delta^2(t, \tau)dt. \tag{10}$$

When $\Delta(t, \tau)$ is a stationary random process, we can write the Allan variance in the equivalent form

$$\sigma_y^2(\tau) = \frac{1}{2} E[\Delta^2(t, \tau)], \tag{11}$$

where E is the expected value. This form is particularly convenient for calculations. We have

$$E[\Delta^2(t, \tau)] = E\left[\bar{y}^2(t)\right] + E[\bar{y}^2(t + \tau)] - 2E\left[\bar{y}(t)\bar{y}(t + \tau)\right]. \tag{12}$$

For the white frequency noise (3), it is

$$E[\Delta^2(t, \tau)] = 2\tau^{-1}, \tag{13}$$

$\sigma_y^2(t,\tau)$	t region	τ region
$a_1^2\tau^{-1}$	$t < -T/2$	$0 < \tau < T/2$
$a_1^2\tau^{-1} + \frac{1}{4}(a_2^2 - a_1^2)\frac{(t+T/2)^2}{T-2\tau}\tau^{-2}$	$-T/2 \le t < -\lvert T/2 - 2\tau\rvert$	$0 < \tau < T/2$
$\frac{1}{2}(a_1^2 + a_2^2)\tau^{-1} + (a_2^2 - a_1^2)\tau^{-1}\frac{t}{T-2\tau}$	$-\lvert T/2 - 2\tau\rvert \le t < \lvert T/2 - 2\tau\rvert$	$0 < \tau \le T/4$
$\frac{1}{2}(a_1^2 + a_2^2)\tau^{-1} + \frac{1}{2}(a_2^2 - a_1^2)\tau^{-2}t$	$-\lvert T/2 - 2\tau\rvert \le t < \lvert T/2 - 2\tau\rvert$	$T/4 < \tau < T/2$
$a_2^2\tau^{-1} - \frac{1}{4}(a_2^2 - a_1^2)\tau^{-2}\frac{(t-T/2)^2}{T-2\tau}$	$\lvert T/2 - 2\tau\rvert \le t < T/2$	$0 < \tau < T/2$
$a_2^2\tau^{-1}$	$t > T/2$	$0 < \tau < T/2$

Table 1. DAVAR of a change of variance in the clock noise.

because

$$E\left[\bar{y}^2(t)\right] = E[\bar{y}^2(t+\tau)] = \tau^{-1}, \quad (14)$$

$$E\left[\bar{y}(t)\bar{y}(t+\tau)\right] = 0. \quad (15)$$

Substituting, we obtain the classic result [10]

$$\sigma_y^2(\tau) = \tau^{-1}. \quad (16)$$

The DAVAR is defined as

$$\sigma_y^2(t,\tau) = \frac{1}{2(T-2\tau)}\int_{t-T/2+\tau}^{t+T/2-\tau} E[\Delta^2(t',\tau)]dt', \quad (17)$$

where T is the length of the analysis window. Replacing (13), we have

$$\sigma_y^2(t,\tau) = \tau^{-1}. \quad (18)$$

Therefore, the DAVAR of a white frequency noise with constant variance is stationary with time and equals at any time the Allan variance. Since the white frequency noise (3) is stationary with time, this result satisfies our intuition.

2.2. Change of variance

We consider the time-varying white frequency noise defined as

$$y(t) = a(t)\xi(t), \quad (19)$$

where

$$a(t) = \begin{cases} a_1, & t < 0, \\ a_2, & t \ge 0. \end{cases} \quad (20)$$

The corresponding discrete-time average frequency deviation is given by

$$y[n] = \frac{a[n]}{T_s}\int_{(n-1)T_s}^{nT_s} \xi(t')dt', \quad (21)$$

where

$$a[n] = \begin{cases} a_1, & n < 0, \\ a_2, & n \ge 0. \end{cases} \quad (22)$$

The mean of $y[n]$ is zero, and its standard deviation is given by

$$\sigma_y[n] = \begin{cases} \frac{a_1}{\sqrt{T_s}}, & n < 0, \\ \frac{a_2}{\sqrt{T_s}}, & n \ge 0. \end{cases} \quad (23)$$

Therefore, a step change in $a(t)$ at $t = 0$ implies a step change in the standard deviation of the measured frequency at $n = 0$.

To compute the term $E[\Delta^2(t,\tau)]$, we see that

$$E\left[\bar{y}^2(t)\right] = \begin{cases} a_1^2\tau^{-1}, & t < 0, \\ a_1^2\tau^{-1} + (a_2^2 - a_1^2)t\tau^{-2}, & 0 \le t < \tau, \\ a_2^2\tau^{-1}, & t \ge \tau. \end{cases} \quad (24)$$

$$E[\bar{y}^2(t+\tau)] = \begin{cases} a_1^2\tau^{-1}, & t < -\tau, \\ a_2^2\tau^{-1} + (a_2^2 - a_1^2)t\tau^{-2}, & -\tau \le t < 0, \\ a_2^2\tau^{-1}, & t \ge 0, \end{cases} \quad (25)$$

and,

$$E\left[\bar{y}(t)\bar{y}(t+\tau)\right] = 0. \quad (26)$$

Substituting in (12),

$$E[\Delta^2(t,\tau)] = \begin{cases} 2a_1^2\tau^{-1}, & t \le -\tau, \\ (a_1^2 + a_2^2)\tau^{-1} + (a_2^2 - a_1^2)t\tau^{-2}, & \lvert t\rvert < \tau, \\ 2a_2^2\tau^{-1}, & t \ge \tau. \end{cases} \quad (27)$$

To compute the Allan variance, we combine (10) and (11), obtaining

$$\sigma_y^2(\tau) = \frac{1}{2}\lim_{T'\to\infty}\frac{1}{T'}\int_{-T'/2}^{T'/2} E[\Delta^2(t,\tau)]dt. \quad (28)$$

After a few calculations, we have

$$\sigma_y^2(\tau) = \frac{a_1^2 + a_2^2}{2}\tau^{-1} \quad (29)$$

Therefore, the Allan variance does not track the nonstationarity in the clock noise variance, since it provides an average of the variance values before and after the step change. Clearly, we cannot use the Allan variance as a tool for characterizing this type of clock anomaly.

By replacing (27) in (17), we obtain the DAVAR shown in Tab. 1. The obtained DAVAR is a function of time, and it actually tracks the change of variance. We discuss its properties in the next section.

3. ANALYSIS OF A CHANGE OF VARIANCE IN THE CLOCK NOISE

As Tab. 1 shows, the obtained DAVAR is a function of the t, τ region considered. When $t < -T/2$ and $t > T/2$ the

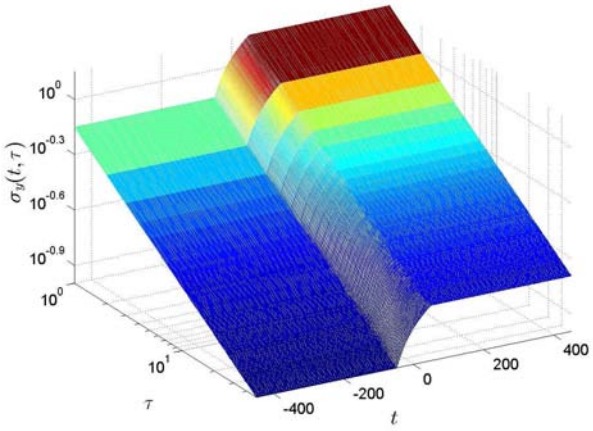

Fig. 2. DADEV of a change of variance. The plot shows the DADEV of a change of variance in the clock noise, obtained when the window length is $T = 100$. Before and after the sudden change of variance, the DADEV surface is stationary with time.

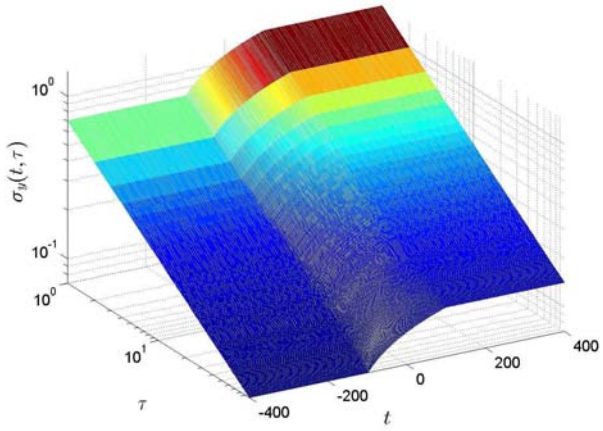

Fig. 3. DADEV of a change of variance for the case of a long window. The plot shows the DADEV of a change of variance in the clock noise obtained for a window length of $T = 200$.

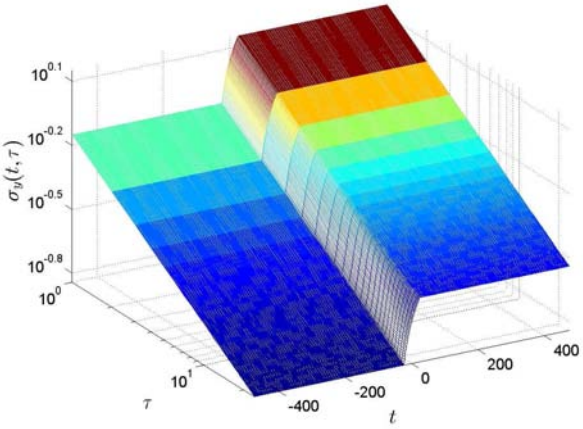

Fig. 4. DADEV of a change of variance for the case of a short window. The plot shows the DADEV of a change of variance in the clock noise obtained for a window length of $T = 50$.

DAVAR is stationary with time and equals the Allan variance of a white frequency noise with a constant variance of $a_1^2\tau^{-1}$ and $a_2^2\tau^{-1}$, respectively. This result is expected because the DAVAR is computed on a sliding window of length T, and hence it catches the change in variance only when $-T/2 \leq t \leq T/2$. In this region, for a given τ, the behavior of the DAVAR is linear or quadratic with time, depending on the time region considered. To better understand this result, we consider a change of variance with parameters $a_1 = 1$ and $a_2 = 2$. In Fig. 2 we show the dynamic Allan deviation (DADEV) obtained for the window length $T = 100$. As commonly done in precise timing, both the observation interval τ and the DADEV are in logarithmic coordinates. Since the DADEV for $t < -T/2$ and $t > T/2$ is proportional to $\tau^{-1/2}$, its representation under this logarithmic scaling is a straight line constant with time. We see that the DADEV correctly tracks the increase in variance occurring at $t = 0$. The change between the two values of variance happens in the transition region $-T/2 \leq t \leq T/2$.

The window length influences the duration of the transition region. Figure 3 shows the DADEV when $T = 200$. We see that the change between the two stationary variance values is much slower than for $T = 100$, corresponding to a poorer localization in time of this clock anomaly. Conversely, in Fig. 4 we show the DADEV for $T = 50$. In this case, the transition region is short and the change of variance is well localized in time. Figures 2-4 clearly highlight the tradeoff on the window length to which the DADEV estimated from measured data is subject. A short window guarantees in fact a good time localization of the change of variance, but will have large fluctuations in the estimates due to the limited number of samples in the window. Conversely, a long window will guarantee lower fluctuations of the estimate, but a poor time localization of the change of variance.

In Fig. 5 we show the DADEV estimated from the GPS data in Fig. 1. The DADEV clearly represents the change of variance in the experimental data. We in fact see the increase in variance at the beginning of the signal, and then, after a block of missing data, the decrease in variance. This low variance value corresponds to the new clock that replaces the malfunctioning one. The fluctuations of the DADEV surface are due to the estimation process.

4. CONCLUSIONS

We have characterized a change of variance in the noise of a precise clock in the DAVAR domain. This anomaly is critical because it can make the clock violate the specifications, and it is potentially associated to major clock failures. We have obtained its exact analytic DAVAR. The result is exact because

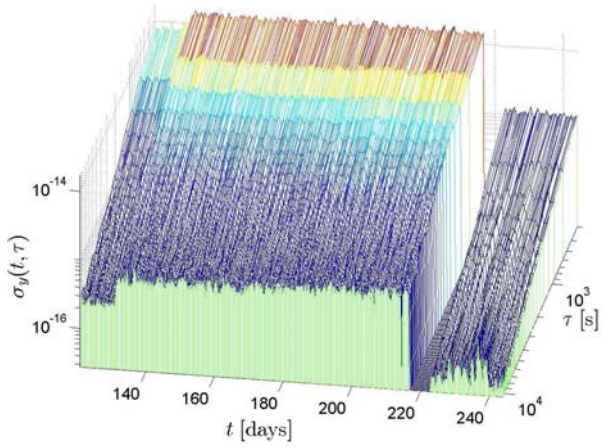

Fig. 5. DADEV of the GPS data shown in Fig. 1. The plot shows the DADEV estimated from the experimental data shown in Fig. 1. The DADEV clearly highlights the changes of variance occurring in the signal. The fluctuations are due to the estimation process.

no approximation has been used. As expected, the DAVAR is stationary with time before and after the anomaly. When the anomaly occurs, the DAVAR shows a transition region which is linear or quadratic with time. This result can be helpful in understanding the health status of a precise clock, an essential problem in GNSSs, and can lead to the design of better automatic anomaly detectors.

5. ACKNOWLEDGEMENTS

We thank Dr. Gianluca Fantino for having provided the GPS data shown in Fig. 1.

REFERENCES

[1] X. Huang, H. Gong, W. Yang, X. Zhu, G. Ou, and J. Zhao, "An Integrity Monitoring Algorithm for Satellite Clock Based on Test Statistics," *China Satellite Navigation Conference (CSNC) 2012 – Lecture Notes in Electrical Engineering*, vol. 160, pp. 515-526, 2012.

[2] Y. J. Heo, J. Cho, and M. B. Heo, "Detection of GPS clock jump using Teager energy operator," *2010 Conference on Precision Electromagnetic Measurements*, 13-18 June 2010, Daejeon, Korea.

[3] S. Lee, J. Kim, M. Jeong, and Y. J. Lee, "Monitoring atomic clocks on board GNSS satellites," *Advances in Space Research*, vol. 47, no. 10, pp. 1654–1663, 2011.

[4] S. Lee J. Kim and Y. J. Lee, "Protecting Signal Integrity Against Atomic Clock Anomalies on Board GNSS Satellites," *IEEE Trans. Instr. Meas.*, vol. 60, no. 7, pp. 2738-2745, 2011.

[5] L. Galleani and P. Tavella, "Detection of atomic clock frequency jumps with the Kalman filter," *IEEE Trans. Ultra. Ferro. Freq. Contr.*, vol. 59, no. 3, pp. 504-509, 2012.

[6] P. Waller, F. Gonzalez, S. Binda, I. Sesia, I. Hidalgo, G. Tobias, and P. Tavella, "The In-Orbit Performances of GIOVE Clocks," *IEEE Trans. Ultra. Ferro. Freq. Contr.*, vol. 57, no. 3, pp. 738-745, 2010.

[7] M. Weiss, P. Shome, and R. Beard, "On-board GPS clock monitoring for signal integrity," *42^{nd} PTTI Meeting*, 15-18 November 2010, Reston, Virginia.

[8] IEEE Standard Definitions of Physical Quantities for Fundamental Frequency and Time Metrology, IEEE Std. 1139-1999.

[9] ITU-R Recommendation TF 538-3, "Measures for random instabilities in frequency and time (phase)," *International Telecommunication Union – Radiocommunication ITU-R*, vol. 2000, TF Series, Geneva, 2001.

[10] D. W. Allan, "Statistics of atomic frequency standards," *Proc. of the IEEE*, vol. 54, no. 2, pp. 221-230, 1966.

[11] D. W. Allan, "Time and Frequency (Time-Domain) Characterization, Estimation, and Prediction of Precision Clocks and Oscillators," *IEEE Trans. Ultra. Ferro. Freq. Contr.*, vol. 34, no. 6, pp. 647-654, 1987.

[12] L. Galleani and P. Tavella, "The Dynamic Allan Variance," *IEEE Trans. Ultra. Ferro. Freq. Contr.*, vol. 56, no. 3, pp. 450-464, 2009.

[13] L. Galleani, "The Dynamic Allan Variance II: A Fast Computational Algorithm," *IEEE Trans. Ultra. Ferro. Freq. Contr.*, vol. 57, no. 1, pp. 182-188, 2010.

[14] L. Galleani, "The Dynamic Allan Variance III: Confidence and Detection Surfaces," *IEEE Trans. Ultra. Ferro. Freq. Contr.*, vol. 58, no. 8, pp. 1550-1558, 2011.

[15] L. Galleani and P. Tavella, "Characterization of atomic clock anomalies in the dynamic Allan variance domain," *IEEE IFCS-EFTF 2013*, 21-25 July 2013, Prague.

[16] I. Sesia, L. Galleani, and P. Tavella, "Application of the Dynamic Allan Variance for the Characterization of Space Clock Behavior," *IEEE Trans. Aero. Elect. Sys.*, vol. 47, no. 2, pp. 884-895, 2011.

[17] P. Kartaschoff, *Frequency and time*, Academic Press, 1978.